Negative regulation of Smad1 pathway and collagen IV expression by store-operated Ca^{2+} entry in glomerular mesangial cells

Running Head: Inhibition of Smad1- collagen IV pathway by SOCE

Peiwen Wu[1,2*], Yuezhong Ren[1,3*], Yuhong Ma[1,4], Yanxia Wang[1], Hui Jiang[1,5], Sarika Chaudhari[1], Mark E. Davis[6], Jonathan E. Zuckerman[6], and Rong Ma[1#]

1: Institute for Cardiovascular and Metabolic Disease
University of North Texas Health Science Center, Fort Worth, Texas 76107

2: Department of Endocrinology, The First Affiliated Hospital of Fujian Medical University, Fuzhou, Fujian, P.R. China

3: Department of Endocrinology, The Second Affiliated Hospital of Zhejiang University College of Medicine, Hangzhou, Zhejiang, China

4: Department of Clinical Medicine, Wannan Medical College, Wuhu, China

5: The First Affiliated Hospital to Anhui University of Traditional Chinese Medicine, Hefei, China

6: Chemical Engineering, California Institute of Technology, Pasadena, CA 91125

*: equally contributed to this work

#: To whom correspondence should be addressed:
3500 Camp Bowie Blvd.
Institute for Cardiovascular and Metabolic Disease
University of North Texas Health Science Center
Fort Worth, TX 76107
Tel: 817-735-2516; Fax: 817-735-5084
E-mail: rong.ma@unthsc.edu

ABSTRACT

Collagen IV (Col IV) is a major component of expanded glomerular extracellular matrix in diabetic nephropathy and Smad1 is a key molecule regulating Col IV expression in mesangial cells (MCs). The present study was conducted to determine if Smad1 pathway and Col IV protein abundance were regulated by store-operated Ca^{2+} entry (SOCE). In cultured human MCs, pharmacological inhibition of SOCE significantly increased the total amount of Smad1 protein. Activation of SOCE blunted high glucose-increased Smad1 protein content. Treating human MCs with angiotensin II at 1 μM for 15 min, or high glucose for 3 days, or TGF-β1 at 5 ng/ml for 30 min increased the level of phosphorylated Smad1. However, the phosphorylation of Smad1 by those stimuli was significantly attenuated by activation of SOCE. Knocking down Smad1 reduced, but expressing Smad1 increased the amount of Col IV protein. Furthermore, activation of SOCE significantly attenuated high glucose-induced Col IV protein production and blockade of SOCE substantially increased the abundance of Col IV. To further verify those *in vitro* findings, we downregulated SOCE specifically in MCs in mice using siRNA against Orai1 (the channel protein mediating SOCE) delivered by the targeted nanoparticle delivery system. Immunohistochemical examinations showed that expression of both Smad1 and Col IV proteins were significantly greater in the glomeruli with positively-transfected Orai1 siRNA compared to the glomeruli from the mice without Orai1 siRNA treatment. Taken together, our results indicate that SOCE negatively regulates the Smad1 signaling pathway and inhibits Col IV protein production in MCs.

ABBREVIATIONS

2-APB: 2-aminoethyl diphenylborinate

Ang II: angiotensin II

Col IV: collagen IV

ER: endoplasmic reticulum

IDV: integrated density value

MC: mesangial cell

NP: nanoparticle

p-Smad1: phospho-Smad1

R-Smad: receptor-regulated Smad

siSmad1: small interfering RNA against human Smad1

SOCE: store-operated Ca^{2+} entry

TG: thapsigargin

63 **KEYWORDS**

64 Store-operated Ca^{2+} entry; collagen IV; Smad1; mesangial cells; extracellular matrix

INTRODUCTION

SOCE, the Ca^{2+} entry through store-operated Ca^{2+} channel driven by depletion of the ER Ca^{2+} is critical to the primary Ca^{2+} signaling pathway in a variety of cell types (35), including glomerular MC (27). This Ca^{2+} signal plays an essential role in a wide variety of physiological functions, such as stimulating exocytosis, regulating gene transcription and protein production, and influencing cell proliferation and apoptosis (35). Recently, emerging evidence suggests that the function of SOCE is cell context dependent. For instance, SOCE contributes to cardiac hypertrophy (19), but suppressed cell growth in mouse embryonic fibroblasts and rat uterine leiomyoma cells (37). This cell-type dependent function of SOCE also exists in kidney. In the proximal tubular epithelial cells, Mai et al reported that blockade of Orai1-mediated SOCE inhibited TGF-β1-stimulated fibronectin protein expression (28). On the contrary, in glomerular MCs we and Mai et al demonstrated that suppression of SOCE increased fibronectin protein abundance (28; 46).

In our recent *in vitro* and *in vivo* studies, we showed that SOCE decreased abundance of MC-derived Col IV (46), one of major extracellular matrix proteins produced by MCs. Because over production of extracellular matrix proteins by MCs and deposition of these proteins to mesangium is an important contributor to mesangial expansion in the early stage of diabetic nephropathy (14; 15), our finding raises a possibility that SOCE pathway could be a potential therapeutic target for diabetic kidney disease. However, the mechanism underlying the inhibitory effect of SOCE is not known yet.

It has been firmly established that Smad signaling pathway plays a crucial role in matrix protein production (23; 24). Smad signaling is initiated with phosphorylation of R-Smad (Smad1, 2, 3, 5, 8) by type I receptors of TGF-β superfamily. Once phosphorylated, R-Smads form heteromeric complexes with Smad4, followed by translocation of the complexes into the nucleus to regulate transcription of target genes. Classically, Smad2/3 stimulates production of fibronectin and connective tissue growth factor (12; 23; 24) while Smad1 promotes Col IV production (3). Smad signaling pathway was recently

89 reported in MCs (2; 3; 10; 30; 38). Particularly, it has been reported that Smad1 signaling pathway was
90 tightly associated with the development of diabetic nephropathy (3; 29; 30). However, the mechanism
91 for regulation and modulation of Smad1 signaling is still unclear. The present study was conducted to
92 test a hypothesis that SOCE inhibited Smad1 pathway and reduced abundance of Col IV, a product of
93 the activated Smad1 pathway.
94

MATERIALS AND METHODS

Materials Information on all antibodies for immunofluorescence experiments was described above. Human recombinant TGFβ1 (240-B-002) was purchased from R&D systems. TG (T-9033), 2-APB (D-9754), lanthanum chloride (449830), and Ang II (A9525) were purchased from Sigma-Aldrich (Sigma, ST. Louis, MO). Mouse anti-Col IV antibody (M61403M) was purchased from Meridian Life Science, Inc. (Memphis, TN). Anti-Smad1 mouse monoclonal antibody (sc-81378 at 1:200), anti-desmin goat polyclonal antibody (sc-7559), anti-synaptopodin goat polyclonal antibody (sc-21537), and anti-α-tubulin primary antibody (sc-5286) were purchased from Santa Cruz (Dallas, TX). Rabbit polyclonal anti-phospho Smad1 antibody (06-702 at 1:1000) was purchased from EMD Millipore Corp. (Billerica, MA). Rabbit polyclonal anti-Orai1 antibody (O-8264) was purchased from Sigma (ST. Louis, MO). Flag-tagged Smad1 expression plasmid was kindly given by Dr. Xia Lin at Baylor College of Medicine (Houston, TX).

MC culture Human MCs belong to Clonetics^{TM} renal MC system and were purchased from Lonza (Catalog #:CC2559, Walkersville, MD). MCs in a 75 cm^2 flask were cultured in 5.6 mM D-glucose DMEM medium (Gibco, Carlsbad, CA) supplemented with 25 mM HEPES, 4 mM glutamine, 1.0 mM sodium pyruvate, 0.1 mM nonessential amino acids, 100 U/ml penicillin, 100 μg/ml streptomycin and 20% fetal bovine serum. When MCs reached ~90% confluence, the cells were split into 60-mm cell culture plates for various treatments as specified in figure legends. In some experiments, MCs were treated with high glucose. In those experiments, the concentration of D-glucose was 25 mM and cells were growth-arrested with 0.5% serum during treatments. Culture media was replaced with fresh media every 2 days. Only subpassage 4-9 MCs were used in the present study.

Transient transfection of human MCs siSmad1 was purchased from Santa Cruz (Catalog #: 29483). The siSmad1 and scrambled control siRNA (both 50 nM) were transfected into human MCs using Dharmafect 2 transfection reagent (Thermo Scientific, Rockford, IL) in serum free DMEM media

following the protocol provided by the manufacturer. Media was changed to 20% fetal bovine serum DMEM media after 6 h. Cells were harvested for Western blot 48 h after transfection. Flag-tagged expression plasmid of Smad1 (Flag-Smad1) and empty vector (pSHAG) were transfected into MCs at 0.5 μg/ml using Lipofectamine and Plus reagent (Invitrogen-BRL, Carlsbad, CA) following the protocols provided by the manufacturer. Cells were harvested 48 h after transfection for immunoblot analysis.

Western blot The whole cell lysates or renal cortical extracts were fractionated by 10% SDS-PAGE, transferred to PVDF membranes, and probed with primary Col IV, Smad1, p-Smad1, Orai1, β-actin, and α-tubulin antibodies. Bound antibodies were visualized with Super Signal West Femto or Pico Luminol/Enhancer Solution (Thermo Scientific, Rockford, IL). The specific protein bands were visualized and captured using an AlphaEase FC Imaging System (Alpha Innotech, San Leandro, CA). The IDV of each band was measured by drawing a rectangle outlining the band using AlphaEase FC software with auto background subtraction. The expression levels of target proteins were quantified by normalization of the IDVs of those protein bands to that of actin or tubulin bands on the same blot.

Animals All procedures were approved by the University of North Texas Health Science Center Institutional Animal Care and Use Committee. Nine male C57BL/6 mice were purchased from Charles River Laboratories (Wilmington, MA). All mice used in this study were between 2 and 3 months of age. The animals were maintained at the animal facility of the University of North Texas Health Science Center under local and National Institutes of Health guidelines.

In Vivo delivery of NP into the kidney of Mice The targeted NP-delivery system was used to deliver siRNA against Orai1 to the kidney of mice as previously described (46). The compositions and formulation of the NP/siRNA complex were described previously (48). Mice were randomly divided into control (n=5) and Orai1–knocked down (n=4) groups. Tail vein injection of NPs containing Cy3-tagged siRNA against mouse Orai1 (NP-Cy3- siOrai1) were given at a dose of 10 mg/kg siRNA in a volume of ~100 μl to the mice in the Orai1–knocked down group. The sense strand sequence of the NP-

Cy3-siOrai1 is 5'-/5Cy3/GGGUUGCUCAUCGUCUUUAGUGC-3'. The mice in the control group were only given unconjugated NPs through the same route at the same injection volume. These intravenous injections were given on day 1 and 3 of the experiment and the mice were euthanized on day 5. Mice were euthanized via intraperitoneal injection of pentobarbital (100 mg/kg body weight). Kidneys were perfused with PBS to wash out the blood. The left renal artery was then ligated and the left kidney was removed for extracting renal cortical proteins. The mouse was then perfused with 4% paraformaldehyde and the right kidney was then removed and fixed in 4% paraformaldehyde. Paraformaldehyde-fixed kidney was embedded in molten paraffin and then, was sectioned at 4-5 μm in thickness (Cryostat 2800 Frigocut-E; Leica Instruments) for immunohistochemical examinations.

Isolating renal cortex and extracting cortical proteins The left kidneys of mice were used to extract renal cortical proteins. Renal cortex was separated from the other region of kidney using a sharp blade and the cortical tissue was minced using two sharp blades. The cortical tissue was then sonicated in a lysis buffer followed by centrifugation at 20817 g for 15 min at 4ºC. The supernatants were collected for Western blot.

Immunofluorescence staining Anti-desmin goat polyclonal antibody (Santa Cruz, Catalog #: sc-7559) and Alexa Fluor 488 donkey anti-goat IgG (Catalog #: A11055, Life Technologies, Eugene, OR) were used to label mouse glomerular MCs. Anti-synaptopodin goat polyclonal antibody (Santa Cruz, catalog #: sc-21537) and Alexa Fluor 488 donkey anti-goat IgG (Catalog #: A11055, Life Technologies, Eugene, OR) was used to label podocytes. Anti-Col IV rabbit polyclonal antibody (Abcam, Catalog#: ab6586) and Alexa Fluor 488 goat anti-rabbit IgG (Catalog #: A11008, Life Technologies, Eugene, OR) were used to stain Col IV. Anti-Smad1 mouse monoclonal antibody (Santa Cruz, Catalog #: sc-81378) and Alexa Fluor 488 goat anti-mouse IgG (Catalog #: A21202, Life Technologies, Eugene, OR) was used to stain Smad1. All primary antibodies were diluted at 1:100 and all secondary Alexa Fluor antibodies were diluted at 1:200. Sections were visualized using an Olympus microscope (BX41) equipped for

epifluorescence and an Olympus DP70 digital camera with DP manager software (version 2.2.1). Sections were coded and viewed by an observer masked to their origins. Images were uniformly adjusted for brightness and contrast and converted to 8-bit format for measuring fluorescence intensity using Image J (version 1.50b, NIH).

Statistical Analysis Data were reported as means ± SE. The one-way ANOVA plus Student-Newman-Keuls post-hoc analysis and Student unpaired t-test were used to analyze the differences among multiple groups and between two groups, respectively. $P<0.05$ was considered statistically significant. Statistical analysis was performed using SigmaStat (Jandel Scientific, San Rafael, CA).

RESULTS

SOCE decreased abundance of Smad1 protein in human MCs.

To determine if SOCE regulated Smad1 signaling, we carried out Western blot and examined effects of inhibition and activation of SOCE on content of Smad1 protein. As shown in Fig. 1 A&B, treating MCs with an SOCE inhibitor, 2-APB (50 μM) significantly increased abundance of Smad1 protein. However, this response was not observed in the cells treated with methanol, the vehicle control of 2-APB.

It was reported that the products of hyperglycemia stimulated synthesis of Smad1 protein in MCs (3). We next examined if SOCE affected high glucose-stimulated Smad1 protein production. Incubation of MCs with high glucose (25 mM) for 3 days significantly increased amount of Smad1 protein (Fig. 1 C&D). However, activation of SOCE by TG (1 μM) in the cells exposed to high glucose for the same time period significantly blunted the Smad1 response (Fig. 1 E&F). These results suggest that SOCE reduced Smad1 protein abundance in human MCs under unstimulated and stimulated (high glucose) conditions.

SOCE inhibited phosphorylation of Smad1 in human MCs.

In addition to reducing the protein amount, suppressing protein activity might be another mechanism for SOCE regulating Smad1 pathway. Like other classical Smad signaling, Smad1 pathway is activated by phosphorylation. It has been reported that Ang II at 1 μM activated Smad1 signaling by phosphorylation of Smad1 in MCs in a time dependent manner, peaking at 15 min (30). We thereby examined if activation of SOCE could inhibit Ang II-induced Smad1 phosphorylation. In agreement with the published study (30), treating human MCs with Ang II at 1 μM for 15 min significantly increased phosphorylated Smad1 without changes in the total amount of Smad1. However, in the presence of TG (1 μM), but not DMSO (1:1000) the Ang II-induced Smad1 phosphorylation was not observed (Fig. 2 A&B).

We next examined if high glucose could also induce phosphorylation of Smad1 and SOCE could also inhibit the phosphorylation. As shown in Fig. 2 C&D, high glucose treatment increased the level of phospho-Smad1. However, the ratio of phospho-Smad1 to the total amount of Smad1 was not significantly increased because high glucose also increased the total amount of Smad1 as shown in Fig. 1 E&F. Interestingly, activation of SOCE with TG resulted in a greater decrease in phospho-Smad1 level than the decrease in the total abundance of Smad1, leading to a significant decrease in ratio of phospho-Smad1 to total Smad1 (Fig. 2 E&F).

It is generally acknowledged that Smad1 transduces bone morphogenetic protein signals (4; 43). However, recent studies demonstrated that TGF-β1 also activated Smad1 pathway in a variety of cells (5; 32). To further determine the inhibitory effect of SOCE on Smad1 activation, we examined if activation of SOCE could decrease TGF-β1-induced phosphorylation of Smad1. As shown in Fig. 3 A&B, treatment of human MCs with 5 ng/ml TGF-β1 significantly increased phospho-Smad1 as early as 30 min after treatment and this response sustained at least for 240 min. However, the total amount of Smad1 had no change during the period of treatment. This TGF-β1-stimulated Smad1 activation was dramatically reduced by TG treatment (Fig. 3 C&D). Furthermore, the inhibitory effect of TG was prevented by 2-APB and La^{3+} (Fig. 3 E&F), suggesting that the inhibition of TG on the TGF-β1/Smad1 pathway was attributed to activation of SOCE, but not by a possible ER stress.

Taken together, the data presented in Figs. 2 and 3 suggest that SOCE inhibited activation of Smad1 signaling in human MCs.

Smad1 increased abundance of Col IV protein in human MCs.

Smad1 has been shown to be a key molecule for direct transcriptional regulation of Col IV in mouse MCs (3). To determine if Smad1 regulates Col IV protein content in human MCs, we manipulated Smad1 expression level and evaluated how it affected Col IV protein abundance in cultured human MCs. We found that knockdown of Smad1 using RNAi approach significantly reduced abundance of Col IV

protein (Fig. 4 A&B). Efficiency of the Smad1 siRNA was indicated by a marked decrease in Smad1 protein content in the cells treated with the siRNA, but not by its scramble control (Fig. 4C). Furthermore, over expression of Smad1 increased Col IV protein content (Fig. 4D). These data, combined with the previous study that Smad1 directly activated transcription of Col IV (3), suggest that production of Col IV is a result of activation of Smad1 pathway in human MCs.

SOCE decreased abundance of Col IV protein produced by human MCs.

The experiments presented above (Fig. 4) showed that activation of Smad1 pathway stimulated Col IV protein production. If SOCE suppressed Smad1 signaling, then this Ca^{2+} signal should inhibit production of Col IV.

High glucose is known to activate Smad1 pathway and stimulate production of Col IV protein by MCs (3; 6; 42). To determine effect of SOCE on Col IV protein production in MCs, we examined if activation of SOCE could inhibit high glucose-induced Col IV response. As shown in Fig. 5 A&B, high glucose (25 mM) treatment for 3 days significantly increased content of Col IV protein in human MCs. This response was abolished by TG (1 μM), but not by its vehicle (DMSO). In agreement with these results, inhibition of SOCE with 50 μM 2-APB or 2 μM lanthanum (La^{3+}) both of which are inhibitors of store-operated Ca^{2+} channel (27; 35), significantly increased Col IV protein abundance. However, this response was not observed in the cells treated with methanol, the vehicle control for 2-APB (Fig. 5 C&D). These data are consistent with our previous study (46) and suggest that SOCE inhibited Col IV protein production by MCs.

***In vivo* suppression of SOCE in MCs increased expression of glomerular Smad1 protein in mice.**

We next carried out animal study to verify our *in vitro* findings. Orai1 is the pore-forming unit of store-operated Ca^{2+} channel (11; 44). Our recent study demonstrated that knocking down Orai1 using siRNA nearly eliminated SOCE in cultured human MCs (8). We thereby speculated that we could inhibit SOCE in MCs *in vivo* by delivery of siRNA against Orai1 to intact animals. Using the targeted *in*

vivo NP/siRNA delivery system (46; 48), we treated mice with Cy3-tagged siRNA against mouse Orai1 (NP-Cy3-siOrai1) which was carried by NPs through tail vein injection using the protocol described in our previous studies (46; 48). Consistent with our previous reports (46; 48), the NP/siRNA complexes were restricted to glomeruli and were not detectable in the surrounding renal tubules or interstitium (Fig. 6A). By labeling MCs with desmin and podocytes with synaptopodin, we further identified that the siRNAs were predominantly localized in MCs, but not in podocytes (Fig. 6B). Western blot of renal cortical extracts showed that Orai1 protein abundance was significantly reduced in the siRNA-treated mice compared to NP alone-treated mice (Fig. 6 C&D). These data suggest that our *in vivo* NP delivery system could deliver functional siRNA specifically to MCs in mice.

We then performed immunofluorescence staining to examine the effect of *in vivo* knockdown of Orai1 specifically in MCs on Smad1 protein expression in mice. Consistent with a published study (18), the expression of Smad1 was only detected in tubules, but not detectable in glomeruli in normal (control) adult mouse (Fig. 7A). However, the glomeruli with Orai1 knocked down in the mice receiving NP-Cy3-siOrai1 showed strong staining of Smad1 (Fig. 7 A&B). Consistently, abundance of Smad1 protein in renal cortex was also significantly increased in the siRNA-treated mice (Fig. 7 C&D). These *in vivo* data are consistent with our *in vitro* data (Fig. 1) and further suggest that SOCE decreased Smad1 protein abundance in MCs.

***In vivo* suppression of SOCE in MCs increased glomerular Col IV protein in mice.**

We also conducted immunohistochemical and biochemical examinations to assess changes in glomerular Col IV protein content in the mice with and without knockdown of Orai1. In the mice treated with NP alone, Col IV staining in glomerulus was mild. However, in the mice receiving NP-Cy3-siOrai1 the immunofluorescence of Col IV in the glomeruli positively transfected with Orai1 siRNA was significantly greater (Fig. 8 A&B). Consistently, abundance of Col IV protein in renal cortex was also

significantly increased in the siRNA-treated mice (Fig. 8 C&D). These data provided *in vivo* evidence that inhibition of SOCE in MCs increased glomerular Col IV protein abundance.

DISCUSSION

Glomerular MCs sit between glomerular capillary loops and maintain the structural architecture of the capillary networks. These cells play important roles in mesangial matrix homeostasis, regulation of glomerular filtration rate and phagocytosis of apoptotic cells in glomerulus (1; 39). MC dysfunction is closely associated with several glomerular diseases, such as diabetic nephropathy (20; 40). Like many other cell types, MC function is largely regulated by intracellular Ca^{2+} signals and the MC Ca^{2+} homeostasis is, at a large extent, attributed to Ca^{2+} channels in the plasma membrane (25). Over past decades, we and others have demonstrated that SOCE mediates MC Ca^{2+} responses to a variety of circulating and locally produced hormones (7; 26; 33). However, the functional roles of SOCE signaling in MC physiology and pathology have remained unclear until recently we demonstrated that this Ca^{2+} entry decreased production of matrix proteins (fibronectin and Col IV) (46). The present study extended our previous findings on the beneficial effects of SOCE. More importantly, this study provided *in vitro* and *in vivo* evidence that Smad1 is involved in the anti-fibrotic effect of SOCE in MCs.

Accumulation of extracellular matrix proteins, including those generated by MCs, is a major pathological change in glomerulus in early stage of diabetic kidney disease (9). Col IV is a major component of increased glomerular extracellular matrix in diabetic nephropathy. During the process of glomerular injuries, MCs can overproduce Col IV (13). Smad1 has been shown to be a key molecule for direct transcriptional regulation of Col IV in MCs (3). In the present study, we also showed that downregulation of Smad1 decreased and upregulation of Smad1 increased Col IV protein abundance in MCs. Thus, our study is consistent with the previous study and suggest existence of an Smad1-Col IV pathway in glomerular MCs.

The most important finding from the present study is that SOCE is a negative regulator of Smad1 signaling. Like other receptor-regulated Smads, Smad1 signaling is initiated with phosphorylation by type I receptors of TGF-β superfamily. The activity of Smad1 pathway can be altered by a change of

either the total protein amount or the phosphorylation state of Smad1. Our data from the present study showed that SOCE inhibited Smad1 signaling through both mechanisms. Inhibition of SOCE both *in vitro* and *in vivo* significantly increased the total amount of Smad1 in cultured MCs and in glomeruli of mice. Activation of SOCE abolished high glucose-induced increase in abundance of Smad1. In addition, activation of SOCE substantially attenuated phosphorylation of Smad1 by Ang II, high glucose, and TGF-β1, all of which are known pathological stimuli in the process of diabetic nephropathy (22; 36; 47).

Recent studies revealed that both glomerular expression of Smad1 and urinary excretion of Smad1 were increased significantly in diabetic rats along with mesangial expansion (30). Further study showed that the increase of urinary Smad1 in the early stage of diabetes was correlated with later development of glomerulosclerosis in two rodent models of diabetic nephropathy (29). Thus, urinary Smad1 could be used as a biomarker for diabetic nephropathy (21; 29) and inhibition of Smad1 pathway should be beneficial to kidney under conditions of diabetes. Our finding that SOCE is an inhibitory mechanism for deleterious Smad1 signaling in MCs suggest that pharmacological and biological increase of SOCE in MCs could protect kidney from diabetic injury and thereby could be a therapeutic option for diabetic kidney disease.

It has been firmly established that TGF-β1 plays the most crucial role in glomerular matrix accumulation in diabetic nephropathy (47). Smad 2/3 is the classical downstream pathway activated by TGF-β1 (2; 24). However, TGF-β1 also activates Smad1 pathway in a variety of cells, including MCs (5; 32). The role of TGF-β1/Smad1 pathway in regulation of extracellular protein expression is cell type- and cell context-dependent. In several cell types, such as endothelial cells, Smad1 signaling counteracts TGF-β1/Smad2/3-induced matrix protein expression (16). However, in hepatic stellate cells and scleroderma fibroblasts, TGF-β1/Smad1 pathway promotes fibrotic phenotype (31; 34; 45). Particularly, the present study and a recent study from other group (5) demonstrated that the TGF-β1/Smad1 pathway promoted matrix protein expression in MCs. Because indiscriminate complete blockade of TGF-β

function does not protect kidney from diabetic injury (41), therapeutic targeting of TGF-β1 requires more optimal strategies such as those selectively directed at specific signaling pathway. Smad1, as a downstream signaling molecule of TGF-β1 and a fibrotic factor in MCs, could be a candidate of this kind of therapeutic targets. The present study suggest that SOCE is an endogenous suppressor of Smad1 signaling and thus manipulation of SOCE in MCs could be a strategy intervening the detrimental Smad1 pathway to ameliorate renal injury in diabetes.

This study has a couple of limitations that must be acknowledged. Firstly, the study is mainly descriptive, limiting the determination of mechanisms by which SOCE suppresses Smad1 pathway. Because our data showed that activation of SOCE decreased both abundance and activity (phosphorylation) of Smad1 protein, multiple mechanisms might be involved in the SOCE inhibitory responses. Regarding inhibition on Smad1 phosphorylation by SOCE, several possibilities exist. At the level of TGF-β receptors, SOCE may inhibit the type II or type I receptor kinase which in turn, suppresses the subsequent phosphorylation of Smad1. Another possibility is that SOCE either activates a Ca^{2+} dependent phosphatase or inhibits a protein kinase which uses Smad1 as its substrate. Alternatively, SOCE could facilitate the interaction between an inhibitory Smad and the TGF-β receptors, leading to inactivation of the downstream Smad1 signaling. Study has shown that the inhibitory Smad is present and functional in MCs (17). Secondly, it is not clear whether inhibition of Smad1 pathway by SOCE is a general mechanism or a MC specific mechanism. In terms of regulation of protein synthesis, the function of SOCE is cell type specific and cell context dependent (19; 37). This is also true in kidney cells. For instance, we and others demonstrated that SOCE inhibited fibronectin and Col IV protein production in glomerular MCs (28; 46), but it increased abundance of the matrix proteins produced by the proximal tubular epithelial cells (28). Thus, the findings in MCs from this study may not be able to extend to other cell types. Despite these limitations, the current studies *in vitro*

and *in vivo* suggest that Smad1 pathway and the matrix protein (Col IV) produced by activation of this pathway are under control of SOCE in MCs.

In summary, we defined a negative regulation of Smad1 signaling pathway and Col IV protein expression by SOCE in MCs. The inhibition on Smad1 signaling was through both decreasing protein content of Smad1 and suppressing phosphorylation of Smad1. Because Smad1 signaling is associated with the development of diabetic kidney disease and over production of Col IV is one of major pathological changes in glomeruli of diabetic kidney, our findings suggest that SOCE in MCs may be an alternative therapeutic option for treating patients with diabetic nephropathy.

ACKNOWLEDGEMENTS

We thank Harry S. Moss Heart Trust for supporting this study and Dr. Xia Lin at Baylor College of Medicine for providing us Flag-tagged Smad1 expression plasmid.

GRANTS

The work was supported by National Institutes of Health (NIH/NIDDK) Grant RO1 (5RO1DK079968-01, to R. Ma), by Grant-in-Aid from American Heart Association Southwestern Affiliate (16GRNT27780043, to R. Ma), by National Natural Science Foundation of China (81400805, to P. Wu), and by Natural Science Foundation of Fujian Province (2016J01449, to P. Wu).

DISCLOSURE

All authors declared no competing interests.

REFERENCES

1. **Abboud HE**. Mesangial cell biology. *Exp Cell Res* 318: 979-985, 2012.
2. **Abdel-Wahab N, Wicks SJ, Mason RM and Chantry A**. Decorin suppresses transforming growth factor-b-induced expression of plasminogen activator inhibitor-1 in human mesangial cells through a mechanism that involves Ca^{2+}-dependent phosphorylation of Smad2 at serine-240. *Biochem J* 362: 643-649, 2002.
3. **Abe H, Matsubara T, Iehara N, Nagai K, Takahashi T, Arai H, Kita T and Doi T**. Type IV collagen is transcriptionally regulated by Smad1 under advanced glycation end product (AGE) stimulation. *J Biol Chem* 279: 14201-14206, 2004.
4. **Anitha M, Shahnavaz N, Qayed E, Joseph I, Gossrau G, Mwangi S, Sitaraman SV, Greene JG and Srinivasan S**. BMP2 promotes differentiation of nitrergic and catecholaminergic enteric neurons thorugh a Smad1-dependent pathway. *Am J Physiol Gastrointest Liver Physiol* 298: G375-G383, 2010.
5. **Araoka T, Abe H, Tominage T, Mima A, Matsubara T, Murakami T, Kishi S, Nagai K and Doi T**. Transcription factor 7-like 2 (TCF7L2) regulates activin receptor-like kinase 1 (ALK1)/Smad1 pathway for development of diabetic nephropathy. *Mol Cell* 30: 209-218, 2010.
6. **Blaes N, pecher C, Mehrenberger M, Cellier E, Praddaude F, Chevalier J, Tack I, Couture R and Girolami JP**. Bradykinin inhibits high glucose- and growth factor-induced collagen synthesis in mesangial cells through the B2-kinin receptor. *Am J Physiol Renal Physiol* 303: F293-F303, 2012.
7. **Campos AH, Calixto JB and Schor N**. Bradykinin induces a calcium-store-dependent calcium influx in mouse mesangial cells. *Nephron* 91: 308-315, 2002.

8. **Chaudhari S, Wu P, Wang Y, Ding Y, Yuan J, Begg M and Ma R**. High glucose and diabetes enhanced store-operated Ca^{2+} entry and increased expression of its signaling proteins in mesangial cells. *Am J Physiol Renal Physiol* 306: F1069-F1080, 2014.
9. **Chavers BM, Bilous RW, Ellis EN, Steffes MW and Mauer SM**. Glomerular lesions and urinary albumin excretion in type I diabetes without overt proteinuria. *N Engl J Med* 320: 966-970, 1989.
10. **Chen Y, Blom IE, Sa S, Goldschmeding R, Abraham DJ and Leask A**. CTGF expression in mesangial cells: involvement of SMADs, MAP kinase, and PKC. *Kidney Int* 62: 1149-1159, 2002.
11. **Deng X, Wang Y, Zhou Y, Soboloff J and Gill DL**. STIM and Orai-dynamic intermembrane coupling to control cellular calcium signals. *J Biol Chem* 284: 22501-22505, 2009.
12. **Feng X and Derynck R**. Specificity and versatility in TGF-b signaling through Smads. *Annu Rev Cell Dev Biol* 21: 659-693, 2005.
13. **Floege J, Johnson RJ, Gordon K, Iida H, Pritzi P, Yoshimura A, Campbell C, Alpers CE and Couser WG**. Increased synthesis of extracellular matrix in mesangial proliferative nephritis. *Kidney Int* 40: 477-488, 1991.
14. **Gooch JL, Barnes JL, Garcia S and Abboud HE**. Calcineurin is activated in diabetes and is required for glomerular hypertrophy and ECM accumulation. *Am J Physiol Renal Physiol* 284: F144-F154, 2003.
15. **Gorin Y, Block K, Hernandez J, Bhandari B, Wagner B, Barnes JL and Abboud HE**. Nox4 NAD(P)H oxidase mediates hypertrophy and fibronectin expression in the diabetic kidney. *J Biol Chem* 280: 39616-39626, 2005.
16. **Goumans MJ, Valdmimarsdottir G, Itoh S, Lebrin F, Larsson J, Mummery C, Karlsson S and ten Dijke P**. Activin receptor-like kinase (ALK)1 is an antagonistic mediator of lateral TGFbeta/ALK5 signaling. *Mol Cell* 12: 817-828, 2003.

17. **Hayashi Y, Katoh T, Asano K, Onozaki A, Sakurai K, Asahi K, Nakayama M and Watanabe T**. Mechanical stretch down-regulates expression of the *Smad6* gene in cultured rat mesangial cells. *Clin Exp Nephrol* 16: 690-696, 2012.

18. **Huang S, Flanders KC and Roberts AB**. Characterization of the mouse Smad1 gene and its expression pattern in adult mouse tissues. *Gene* 258: 43-53, 2000.

19. **Hulot JS, Fauconnier J, Ramanujam D, Chaanine A, Aubart F, Sassi Y, Merkle S, Cazorla O, Ouillé A, Dupuis M, Hadri L, Jeong D, Mühlstedt S, Schmitt J, Braun A, Bénard L, Saliba Y, Laggerbauer B, Nieswandt B, Lacampagne A, Hajjar RJ, Lompré AM and Engelhardt S**. Critical role for stromal interactionmolecule 1 in cardiac hypertrophy. *Circulation* 124: 796-805, 2011.

20. **Kashgarian M and Sterzel RB**. The pathobiology of the mesangium. *Kidney Int* 41: 524-529, 1992.

21. **Kato H, Si H, hostetter T and Susztak K**. Smad1 as a biomarker for diabetic nephropathy. *Diabetes* 57: 1459-1460, 2008.

22. **Kennefick TM and Anderson S**. Role of angiotensin II in diabetic nephropathy. *Semin Nephrol* 17: 441-447, 1997.

23. **Lan HY**. Diverse roles of TGF-beta/Smads in renal fibrosis and inflammation. *Int J Biol Sci* 7: 1056-1067, 2011.

24. **Lan HY**. Transforming growth factor-b/Smad signalling in daibetic nephropathy. *Clin Exp Pharmacol Physiol* 39: 731-738, 2012.

25. **Ma R, Pluznick JL and Sansom SC**. Ion channels in mesangial cells: function, malfunction, or fiction. *Physiology* 20: 102-111, 2005.

26. **Ma R and Sansom SC**. Epidermal growth factor activates store-operated calcium channels in human glomerular mesangial cells. *J Am Soc Nephrol* 12: 47-53, 2001.

27. **Ma R, Smith S, Child A, Carmines PK and Sansom SC**. Store-operated Ca^{2+} channels in human glomerular mesangial cells. *Am J Physiol* 278: F954-F961, 2000.

28. **Mai X, Shang J, Liang S, Yu B, Yuan J, Lin Y, Luo R, Zhang F, Liu Y, Lv X, Li C, Liang X, Wang W, and Zhou J**. Blockade of Orai1 store-operated calcium entry protects against renal fibrosis. *J Am Soc Nephrol* 27, 3063-3078. 2016.

29. **Mima A, Arai H, Matsubara T, Abe H, Nagai K, Tamura Y, Torikoshi K, Araki M, Kanamori H, Takahashi T, Tominaga T, Matsuura M, Iehara N, Fukatsu A, Kita T and Doi T**. Urinary smad1 is a novel marker to predict later onset of mesangial matrix expansion in diabetic nephropathy. *Diabetes* 57: 1712-1722, 2008.

30. **Mima A, Matsubara T, Arai H, Abe H, Nagai K, Kanamori H, Sumi E, Takahashi T, Iehara N, Fukatsu A, Kita T and Doi T**. Angiotensin II-dependent Src and Smad1 signaling pathway is crucial for the development of diabetic nephropathy. *Lab Invest* 86: 927-939, 2006.

31. **Morris E, Chrobak I, Bujor A, Hant F, Mummery C, ten Dijke P and Trojanowska M**. Endoglin promotes TGF-b/Smad1 signaling in scleroderma fibroblasts. *J Cell Physiol* 226: 3340-3348, 2011.

32. **Muñoz-Félix JM, González-Núñez M and López-Novoa J**. ALK1-Smad1/5 signaling pathway in fibrosis development: friend or foe? *Cytokine Growth Factor Rev* 24: 523-537, 2013.

33. **Nutt LK and O'Neil RG**. Effect of elevated glucose on endothelin-induced store-operated and non-store-operated calcium influx in renal mesangial cells. *J Am Soc Nephrol* 11: 1225-1235, 2000.

34. **Pannu J, Nakerakanti S, Smith E, ten Dijke P and Trojanowska M**. Transforming growth factor-beta receptor type I-dependent fibrogenic gene program is mediated via activation of Smad1 and ERK1/2 pathways. *J Biol Chem* 282: 10405-10413, 2007.

35. **Parekh AB and Putney JW**. Store-operated calcium channels. *Physiol Rev* 85: 757-810, 2005.

36. **Park MJ, Kim D, Lim SK, Choi JH, Han HJ, Yoon KC and Park SH**. High glucose-induced O-GlcNAcylated carbohydrate response element-binging protein (ChREBP) mediates mesangial cell lipogenesis and fibrosis, the possible role in the development of diabetic nephropathy. *J Biol Chem* 289: 13519-13530, 2014.

37. **Peng H, Liu J, Chen R, Wang Y, Duan J, Li C, Li B, Jing Y, Chen X, Mao Q, Xu KF, Walker CL, Li J, Wang J and Zhang H**. mTORC1 enhancement of STIM1-mediated store-operated Ca^{2+} entry constrains tuberous sclerosis complex-related tumor development. *Oncogene* 32: 4702-4711, 2013.

38. **Runyan CE, Schnaper HW and Poncelet AC**. Smad3 and PKCd mediate TGF-b1-induced collagen I expression in human mesangial cells. *Am J Physiol Renal Physiol* 285: F413-F422, 2003.

39. **Schlöndorff D and Bana B**. The mesangial cell revisited: no cell is an island. *J Am Soc Nephrol* 20: 1179-1187, 2009.

40. **Scindia YM, Deshmukh US and Bagavant H**. Mesangial pathology in glomerular disease: targets for therapeutic intervention. *Adv Drug Deliv Rev* 62: 1337-1343, 2010.

41. **Sureshbabu A, Muhsin SA and Choi ME.** TGF-b signaling in the kidney: pro-fibrotic and protective efects. Am J Physiol Renal Physiol 310, F596-F606. 2016.

42. **Tahara A, Tsukada J, Tomura Y, Yatsu T and Shibasaki M**. Effects of high glucose on AVP-induced hyperplasia, hypertrophy, and type IV collagen synthesis in cultured rat mesangial cells. *Endocr Res* 37: 216-227, 2012.

43. **Tripurani SK, Cook RW, Eldin KW and Pangas SA**. BMP-specific SMADs function as novel repressors of PDGFA and modulate its expression in ovarian granulosa cells and tumors. *Oncogene* 32: 3877-3885, 2013.

44. **Wang Y, Deng X and Gill DL**. Calcium signaling by STIM and Orai: intimate coupling details revealed. *Sci Signal* 3: pe42-1-pe42-4, 2010.

45. **Wiercinska E, Wickert L, Denecke B, Said HM, Hamzavi J, Gressner AM, Thorikay M, ten Dijke P, Mertens PR, Breitkopf K and Dooley S**. Id1 is a critical mediator in TGF-beta-induced transdifferentiation of rat hepatic stellate cells. *Hepatol* 43: 1032-1041, 2006.

46. **Wu P, Wang Y, Davis ME, Zuckerman JE, Chaudhari S, Begg M and Ma R**. Store-operated Ca^{2+} channel in mesangial cells inhibits matrix protein expression. *J Am Soc Nephrol* 26: 2691-2702, 2015.

47. **Ziyadeh FN and Sharma K**. Role of transforming growth factor-b in diabetic glomerulosclerosis and renal hypertrophy. *Kidney Int* 48: S34-S36, 1995.

48. **Zuckerman JE, Gale A, Wu P, Ma R and Davis ME**. siRNA delivery to the glomerular mesangium using polycationic cyclodextrin nanoparticles containing siRNA. *Nucl Acid Ther* 25: 53-64, 2015.

FIGURE LEGENDS

Fig. 1. Western blot, showing effect of SOCE on Smad1 protein content in human MCs.

A and **B**: Inhibition of SOCE increased Smad1 protein abundance. **A**: Representative western blots. Cultured human MCs were without treatment (UT) or treated with methanol (Meth) (1:1000, vehicle control for 2-APB) and 2-APB (50 μM) for 2 days. L: protein ladder. Tubulin (TB): loading control. **B:** Summary data from the experiments presented in A. * denotes P<0.05, 2-APB vs. both UT and Meth groups. **C** and **D:** High glucose treatment increased Smad1 protein abundance. **C:** Representative western blots. L: protein ladder. Tubulin (TB): loading control. Confluent human MCs were cultured in serum free medium containing normal glucose (NG, 5.6 mM D-glucose + 20 mM mannitol) or high glucose (HG, 25 mM D-glucose) for 1 day (1D) and 3 days (3D). **D:** Summary data from the experiments presented in C. * denotes P<0.05, compared to NG group at the same time point. "n" indicates the number of independent experiments. **E** and **F:** Activation of SOCE inhibited high glucose-stimulated Smad1 production. **E:** Representative western blots. L: protein ladder. Tubulin (TB): loading control. Confluent human MCs were cultured in serum free medium containing normal glucose (NG, 5.6 mM D-glucose + 20 mM mannitol) or high glucose (HG, 25 mM D-glucose) for 3 days. In two groups with high glucose treatment, DMSO (1:1000, vehicle control) and TG (1 μM) were applied on day 2. **F:** Summary data from the experiments presented in E. * denotes P<0.05, compared to NG group. † denotes P<0.05, compared to both HG and HG+DMSO groups. "n" indicates the number of independent experiments.

Fig. 2. Western blot, showing inhibition of phosphorylation of Smad1 by SOCE in human MCs

A and **B:** Activation of SOCE inhibited Ang II-induced phosphorylation of Smad1. **A:** Representative Western blot, showing changes in abundance of phosphorylated Smad1 (p-Smad1) and total Smad1 (T-Smad1) proteins in different treatment groups. Human MCs were without treatment (UT) or treated with Ang II (1 μM) for 15 min in the presence of DMSO (1:1000, vehicle control for TG) or

TG (1 μM). L: a protein ladder. **B:** summary data from the experiments presented in A, showing the ratio of p-Smad1 to T-Smad1 in different groups. * denotes $p<0.05$, vs UN; † denotes $p<0.05$; vs. both Ang II and Ang II + DMSO. "n" indicates the number of independent experiments. **C** and **D:** Activation of SOCE inhibited high glucose-induced phosphorylation of Smad1. **C:** Representative western blots, showing changes in abundance of phosphorylated Smad1 (p-Smad1) and total Smad1 (T-Smad1) proteins in different treatment groups. Serum-deprived human MCs were cultured in normal glucose (NG, 5.6 mM D-glucose + 20 mM mannitol) or high glucose (HG, 25 mM D-glucose) for 3 days. In two groups with high glucose treatment, DMSO (1:1000, vehicle control) and TG (1 μM) were applied on day 2. L: protein ladder. **D:** Summary data from the experiments presented in C, showing the ratio of p-Smad1 to T-Smad1 in different groups. * denotes $P<0.05$, compared to both HG and HG+DMSO groups. "n" indicates the number of independent experiments.

Fig. 3. SOCE inhibited TGF-β1-induced phosphorylation of Smad1 in human MCs.

A and **B:** TGF-β1 phosphorylated Smad1. **A:** Representative Western blot, showing changes in abundance of phosphorylated Smad1 (p-Smad1) and total Smad1 (T-Smad1) in MCs treated with recombinant human TGF-β1 (5 ng/ml) for 0 to 240 min. **B:** summary data from the experiments presented in A, showing the ratio of p-Smad1 to T-Smad1 at different treatment time periods. * denotes $p<0.05$, vs group of 0 min. "n" indicates the number of independent experiments. **C** and **D:** Activation of SOCE inhibited TGF-β1-induced phosphorylation of Smad1. **C:** Representative Western blots, showing changes in abundance of phosphorylated Smad1 (p-Smad1) and total Smad1 (T-Smad1) in different groups. Serum-deprived human MCs were without treatment (UT) or treated with TGF-β1 (5 ng/ml for 30 min) in the presence of DMSO (1:1000) or TG (1 μM). **D:** Summary data from the experiments presented in C, showing the ratio of p-Smad1 to T-Smad1 in different groups. * denotes $P<0.05$, compared to UT; † denotes $P<0.05$, compared to both TGF-β1 and TGF-β1 + DMSO. "n" indicates the number of independent experiments. **E** and **F:** Inhibition of TG on TGF-β1-induced

phosphorylation of Smad1 was due to activation of SOCE. **E:** Representative Western blots, showing the abundance of phosphorylated Smad1 (p-Smad1) and total Smad1 (T-Smad1) in serum-deprived human MCs treated with TGF-β1 (5 ng/ml for 30 min) in the absence or presence of TG (1 μM) with and without 2-APB (50 μM) or La^{3+} (2 μM). **F:** Summary data from the experiments presented in E, showing the ratio of p-Smad1 to T-Smad1 in different groups. * denotes P<0.05, compared to TGF-β1; † denotes P<0.05, compared to TGF-β1 + TG. "n" indicates the number of independent experiments.

Fig. 4. Smad1 increased Col IV protein abundance in human MCs

A: Representative Western blot, showing Col IV protein content in human MCs without transfection (UTran) and the cells transfected with scramble siRNA (Scram) or siRNA against human Smad1 (siSmad1). α-tubulin (TB) was used as a loading control. L: protein ladder. **B:** Summary data from the experiments presented in A. Col IV abundance in each group was normalized to TB and the values in each group were further normalized to that of Utran group. * denotes P<0.05, compared to both Utran and Scram groups. "n" indicates the number of independent experiments. **C:** Representative Western blot from 3 independent experiments, showing Smad1 protein content in human MCs without transfection (UTran) and the cells transfected with Scramble siRNA (Scram) or siRNA against Smad1 (siSmad1). β-actin was used as a loading control. L: protein ladder. **D:** Representative western blot from 3 independent experiments, showing abundance of Smad1 and Col IV proteins in human MCs without transfection (UTran) and the cells transfected with an empty vector (pSHAG) or Flag-tagged Smad1 expresion plasmid (Flag-Smad1). α-tubulin (TB) was used as a loading control. L: protein ladder.

Fig. 5. SOCE decreased abundance of Col IV protein produced by human MCs.

A and **B**: Effect of activation of SOCE on high glucose-stimulated Col IV protein production. **A**: Representative Western blots. L: protein ladder. Tubulin (TB): loading control. **B:** Summary data from the experiments presented in A. Human MCs were cultured in medium containing normal glucose (NG, 5.6 mM D-glucose + 20 mM mannitol) or high glucose (HG, 25 mM D-glucose) with or without DMSO

(1:1000, vehicle control) and TG (1 μM). MCs were with and without various treatments for 2 days in 0.5% FBS medium. In B, * denotes P<0.05, compared to NG group and † denotes P<0.05, compared to both HG and HG+DMSO groups. "n" indicates the number of independent experiments. **C** and **D:** Effect of inhibition of SOCE on Col IV protein production in human MCs. **C:** Representative Western blots. L: protein ladder. Tubulin (TB): loading control. **D:** Summary data from the experiments presented in C. UT: untreated cells; Meth: methanol, vehicle control for 2-APB. Serum starved cells (in 0.5% FBS) were with or without treatments with methanol (1:1000), or 2-APB (50 μM) or La^{3+} (5 μM) for 2 days before harvested. In **D**, * denotes P<0.05, compared to both UT and Meth groups. "n" indicates the number of independent experiments.

Fig. 6. Distribution of NP-Cy3-siOrai1 in mouse kidney

A: Representative images from 4 mice, showing localization of NP-Cy3-siOrai1 (red) in glomeruli (indicated by arrows). Original magnification: 200X. **B:** Localization of NP-Cy3-siOrai1 in MCs (upper panels), but not in podocytes (bottom panels), representative from 4 mice. MCs were stained with desmin (green) and podocytes were stained with synaptopodin (green). NP-Cy3-siOrai1 was shown as red signals. Original magnification: 200X. **C:** Representative Western blot of renal cortical extracts, showing Orai1 protein abundance in the mouse treated with NP alone (NP-Con) and NP containing siRNA against Orai1 (NP-siOrai1). L: protein ladder; Tubulin (TB): loading control. **D:** Summary data. * denotes P<0.05, compared to NP-Con; "n" indicates the number of mice each group.

Fig. 7. *In vivo* knockdown of Orai1 in MCs increased glomerular Smad1 protein in mice.

A: Representative images of Immunofluorescence staining, showing glomerular Smad1 in the mouse treated with NP alone (NP-Con) and NP-Cy3-siOrai1 (knockdown of Orai1). Smad1 is shown as green signals. In the panels of NP-Con, a bright field image was captured to show glomeruli. In the panels of NP-Cy3-siOrai1, the distribution of NP-Cy3-siOrai1 is indicated by Cy3 signals (red). Arrows indicate glomeruli. Original magnification: 200X. **B:** Integrated density (ID) of Smad1 fluorescence averaged

from 4 NP-Con mice and 4 NP-Cy3-siOrai1-treated mice. ** denotes P<0.01, compared to NP-Con. The numbers in parentheses under each bar represent the number of glomeruli counted from 5 sections per kidney. **C** and **D:** Western blot, showing Smad1 protein abundance in the cortex of kidney from the mouse treated with NP alone (NP-Con) and NP-Cy3-siOrai1 (NP-siOrai). **C:** Representative blot. L: protein ladder; TB: α-tubulin, a loading control. **D:** summary data. * denotes P<0.05, compared to NP-Con. "n" indicates the number of mice each group.

Fig. 8. *In vivo* knockdown of Orai1 in MCs increased glomerular Col IV protein in mice.

A: Representative images of Immunofluorescence staining, showing glomerular Col IV in the mouse treated with NP alone (NP-Con) and NP-Cys-siOrai1 (knockdown of Orai1). Col IV is shown as green signals. In the panels of NP-Con, a bright field image was captured to show glomeruli. In the panels of NP-Cy3-siOrai1, the distribution of NP-Cy3-siOrai1 is indicated by Cy3 signals (red). Arrows indicate glomeruli. Original magnification: 200X. **B:** Integrated density (ID) of Smad1 fluorescence averaged from 4 NP-Con mice and 4 NP-Cy3-siOrai1-treated mice. ** denotes P<0.01, compared to NP-Con. The numbers in parentheses under each bar represent the number of glomeruli counted from 5 sections per kidney. **C** and **D:** Western blot, showing Smad1 protein abundance in the cortex of kidney from the mouse treated with NP alone (NP-Con) and NP containing siRNA against Orai1 (NP-siOrai1). **C:** Representative blot. L: protein ladder; TB: α-tubulin, a loading control. **D:** summary data. * denotes P<0.05, compared to NP-Con. "n" indicates the number of mice each group.

Fig. 1

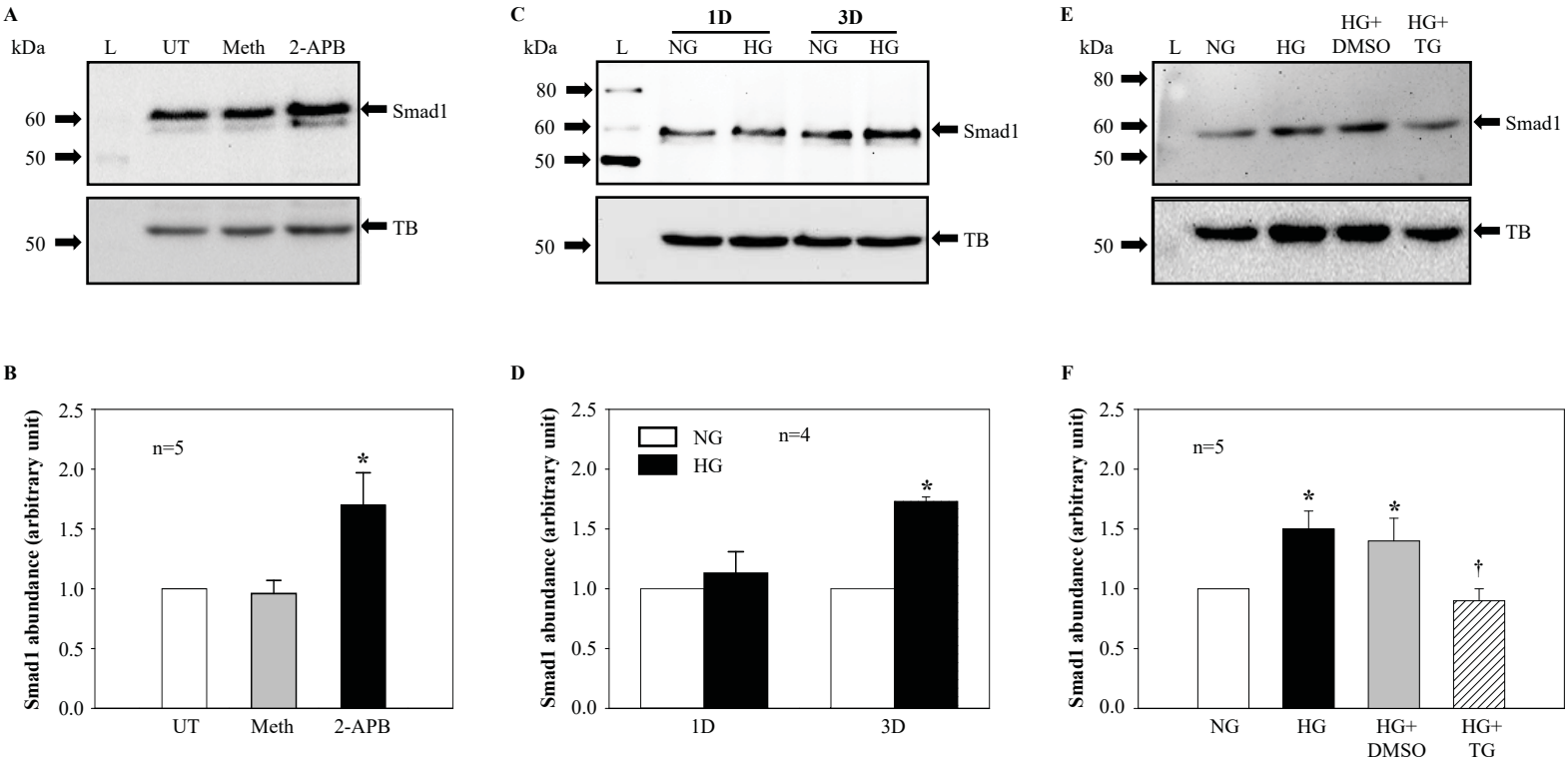
A
kDa
L
UT
Meth
2-APB
60
50
Smad1
50
TB
C
1D
3D
kDa
L
NG
HG
NG
HG
80
60
50
Smad1
50
TB
E
kDa
L
NG
HG
HG+ DMSO
HG+ TG
80
60
50
Smad1
50
TB
B
Smad1 abundance (arbitrary unit)
n=5
*
UT
Meth
2-APB
D
Smad1 abundance (arbitrary unit)
NG
HG
n=4
*
1D
3D
F
Smad1 abundance (arbitrary unit)
n=5
*
*
†
NG
HG
HG+ DMSO
HG+ TG

Fig. 2

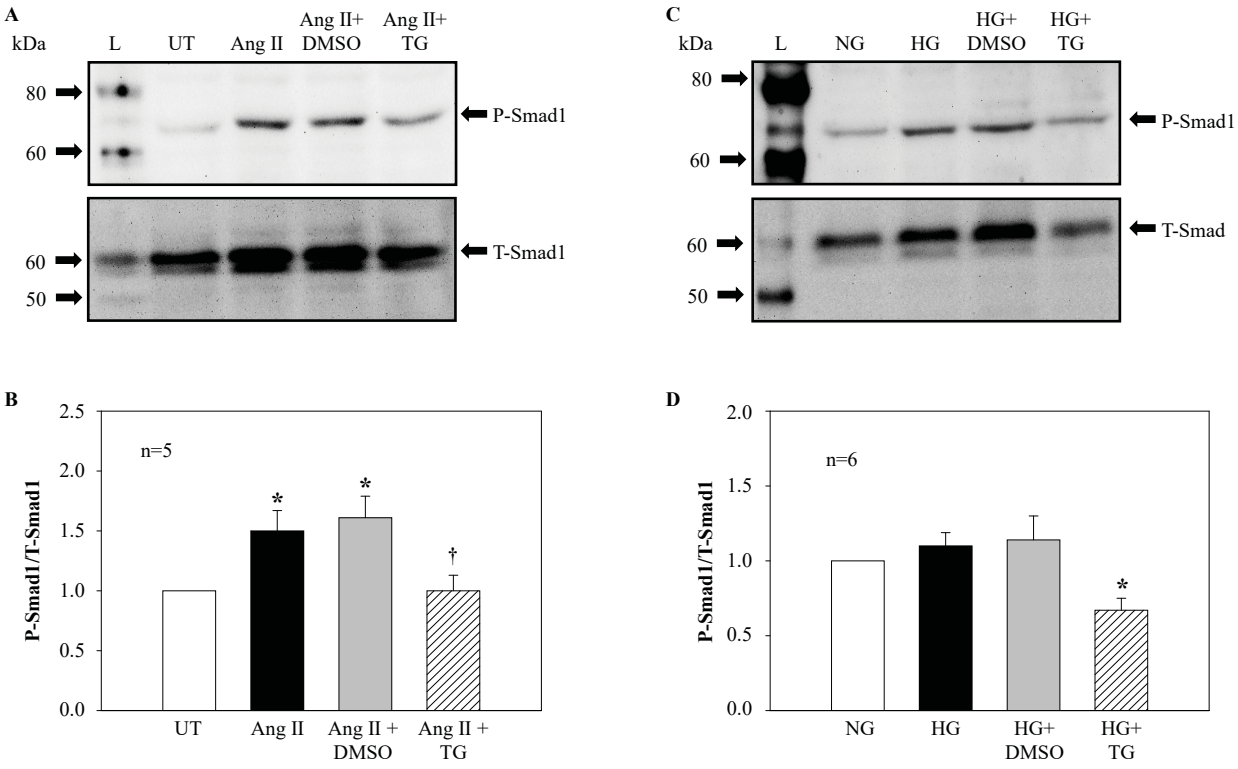
A
kDa
L
UT
Ang II
Ang II+ DMSO
Ang II+ TG
80
60
P-Smad1
60
50
T-Smad1
C
kDa
L
NG
HG
HG+ DMSO
HG+ TG
80
60
P-Smad1
60
50
T-Smad
B
n=5
P-Smad1/T-Smad1
2.5
2.0
1.5
1.0
0.5
0.0
*
*
†
UT
Ang II
Ang II + DMSO
Ang II + TG
D
n=6
P-Smad1/T-Smad1
2.0
1.5
1.0
0.5
0.0
*
NG
HG
HG+ DMSO
HG+ TG

Fig. 3

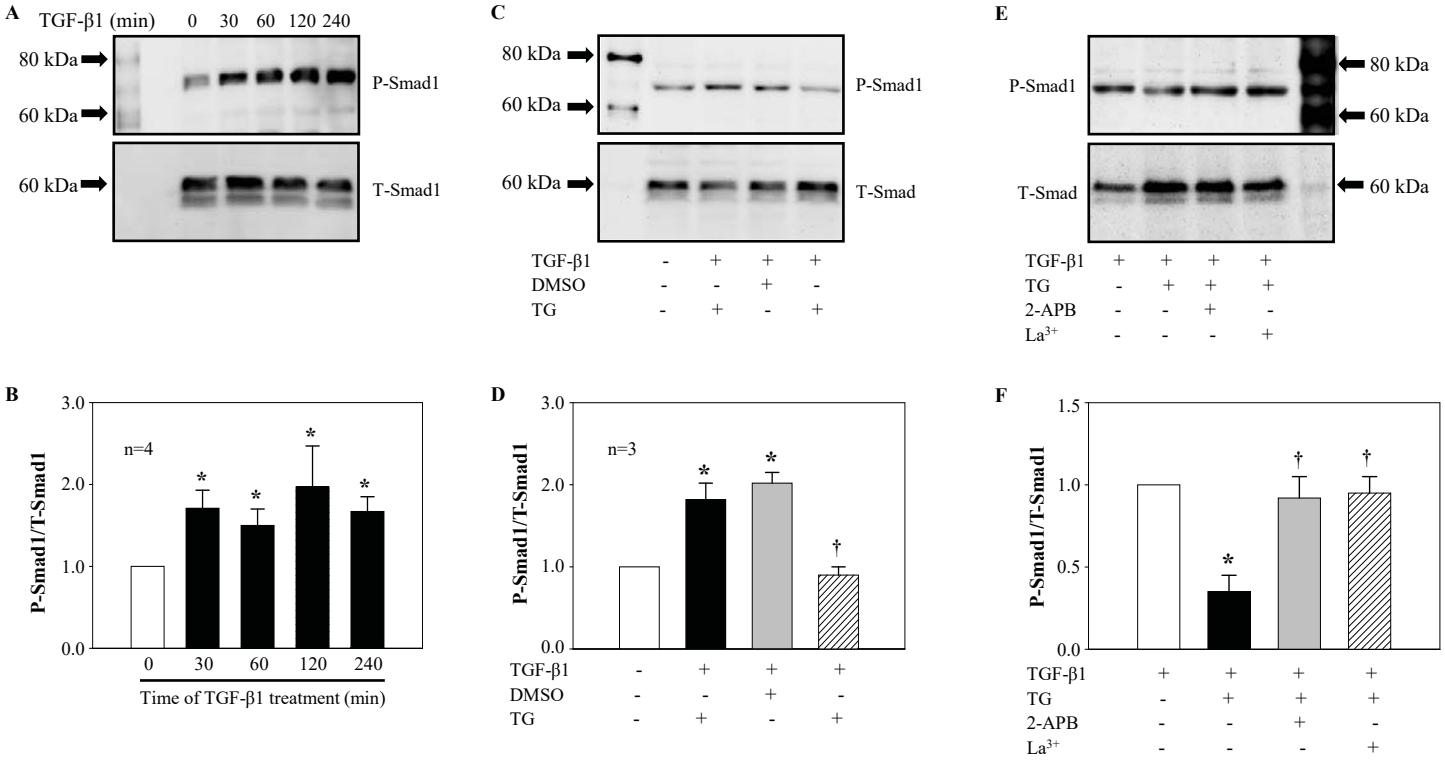
A
TGF-β1 (min) 0 30 60 120 240
80 kDa
60 kDa
P-Smad1
60 kDa
T-Smad1
B
P-Smad1/T-Smad1
n=4
Time of TGF-β1 treatment (min)
C
80 kDa
60 kDa
P-Smad1
60 kDa
T-Smad
TGF-β1
DMSO
TG
D
P-Smad1/T-Smad1
n=3
E
P-Smad1
T-Smad
80 kDa
60 kDa
60 kDa
TGF-β1
TG
2-APB
La3+
F
P-Smad1/T-Smad1

Fig. 4

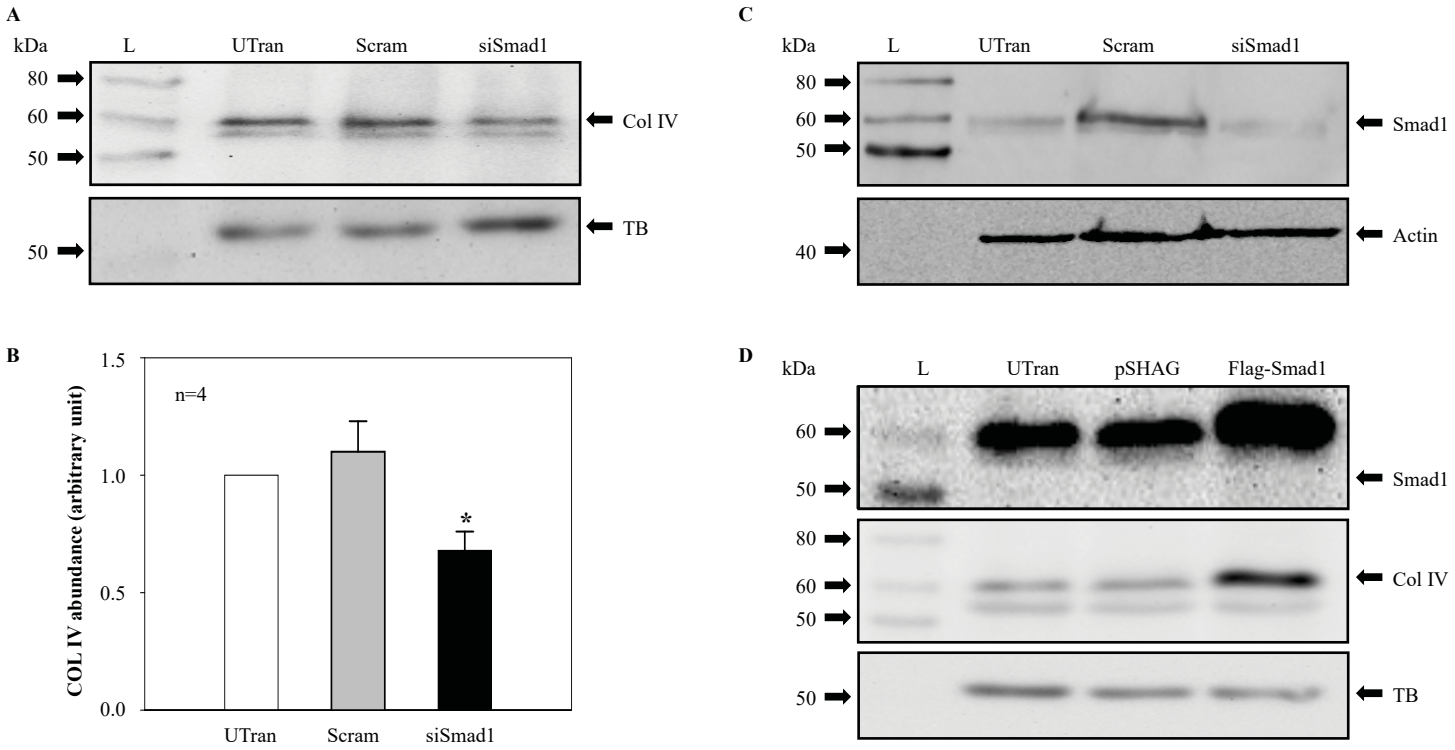
A
kDa
L
UTran
Scram
siSmad1
80
60
50
Col IV
50
TB
C
kDa
L
UTran
Scram
siSmad1
80
60
50
Smad1
40
Actin
B
COL IV abundance (arbitrary unit)
1.5
1.0
0.5
0.0
n=4
*
UTran
Scram
siSmad1
D
kDa
L
UTran
pSHAG
Flag-Smad1
60
50
Smad1
80
60
50
Col IV
50
TB

Fig. 5

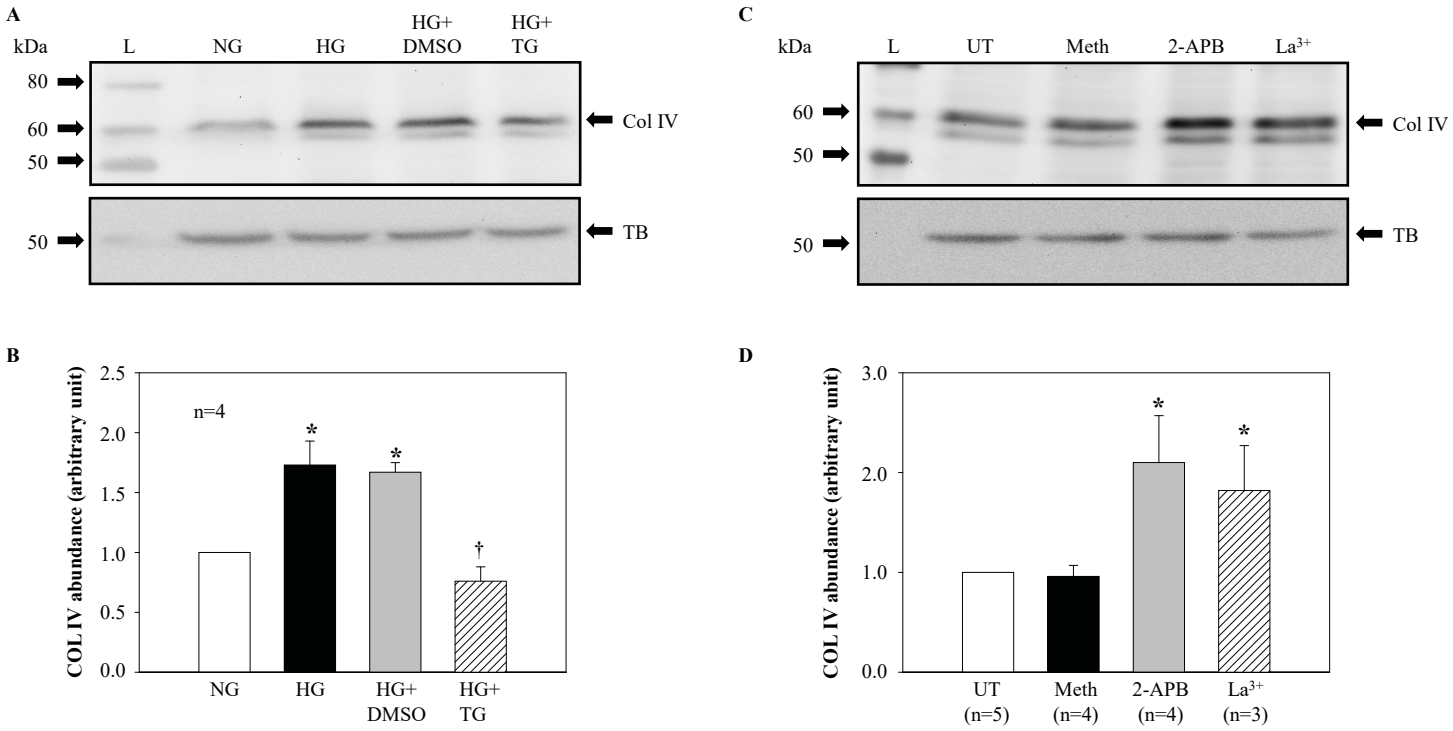
A
kDa
L
NG
HG
HG+ DMSO
HG+ TG
80
60
50
Col IV
50
TB
C
kDa
L
UT
Meth
2-APB
La3+
60
50
Col IV
50
TB
B
COL IV abundance (arbitrary unit)
n=4
NG
HG
HG+ DMSO
HG+ TG
D
COL IV abundance (arbitrary unit)
UT (n=5)
Meth (n=4)
2-APB (n=4)
La3+ (n=3)

Fig. 6

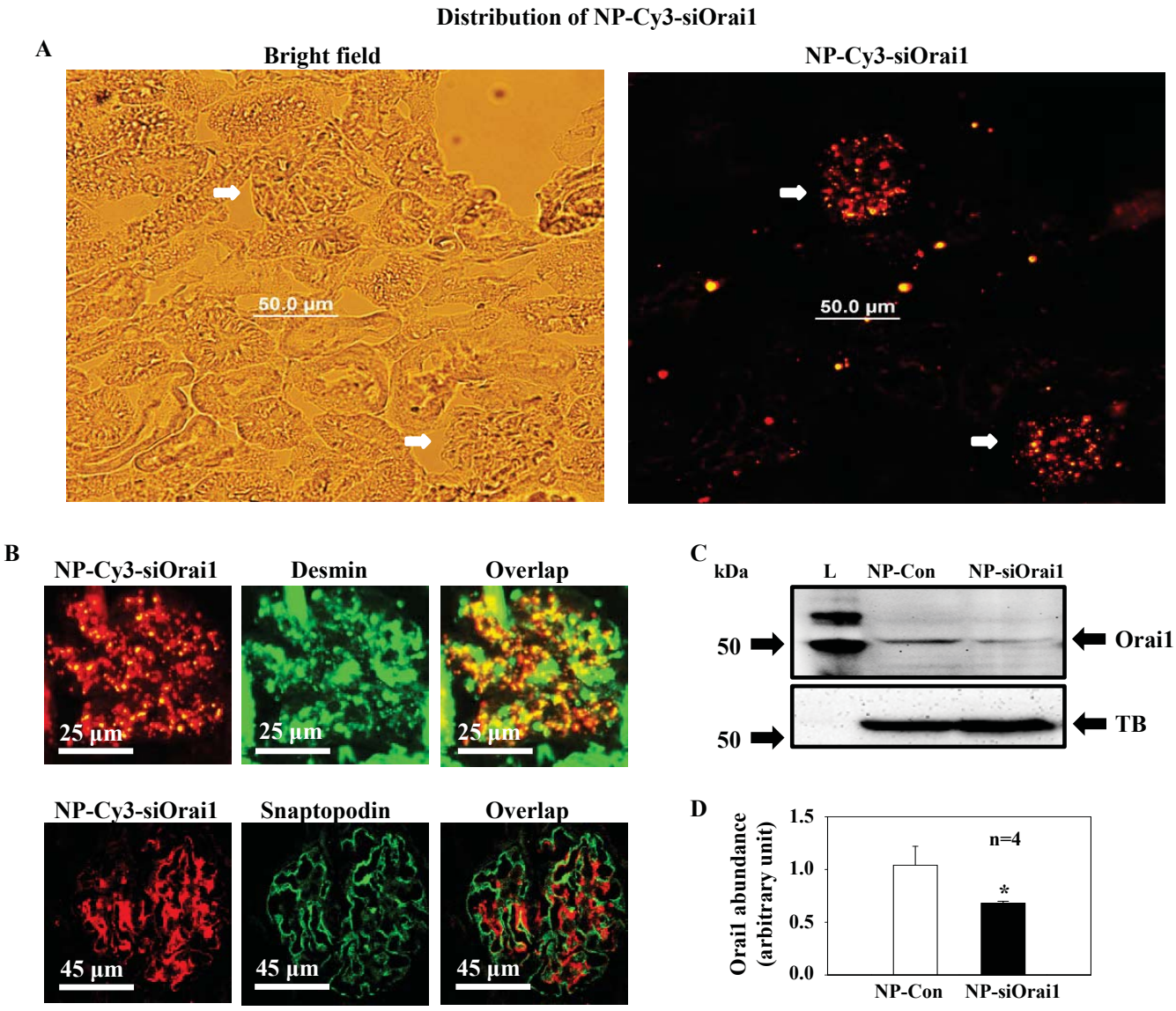
Distribution of NP-Cy3-siOrai1
A
Bright field
NP-Cy3-siOrai1
50.0 μm
50.0 μm
B
NP-Cy3-siOrai1
Desmin
Overlap
25 μm
25 μm
25 μm
NP-Cy3-siOrai1
Snaptopodin
Overlap
45 μm
45 μm
45 μm
C
kDa
L
NP-Con
NP-siOrai1
50
50
Orai1
TB
D
Orai1 abundance (arbitrary unit)
1.5
1.0
0.5
0.0
n=4
*
NP-Con
NP-siOrai1

Fig. 7

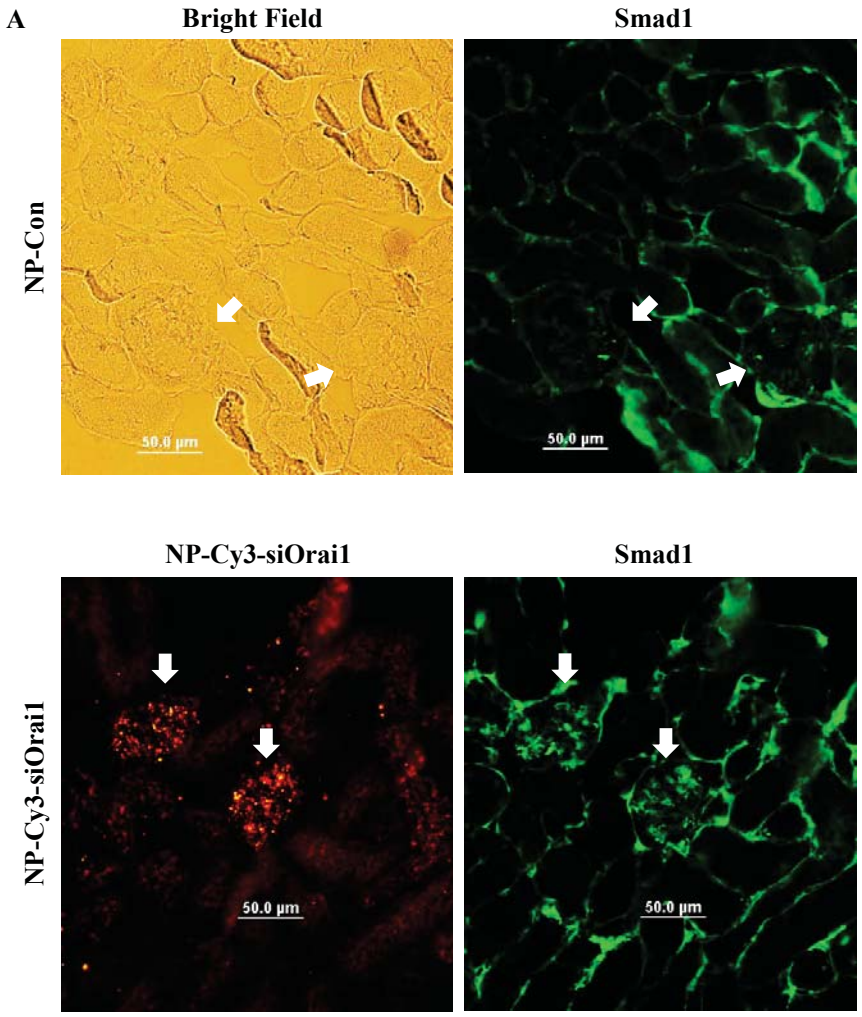
A
Bright Field
Smad1
NP-Con
NP-Cy3-siOrai1
Smad1
50.0 μm
50.0 μm
50.0 μm
50.0 μm

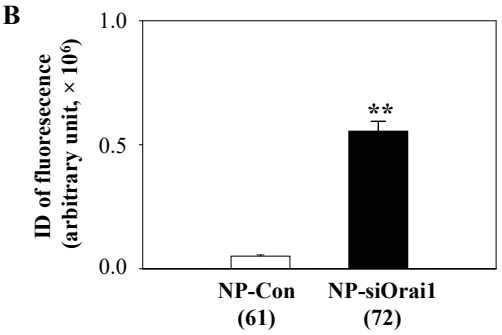
B
ID of fluoresecence (arbitrary unit, × 10⁶)
1.0
0.5
0.0
**
NP-Con (61)
NP-siOrai1 (72)

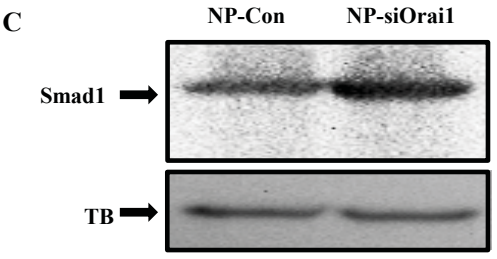
C
NP-Con
NP-siOrai1
Smad1
TB

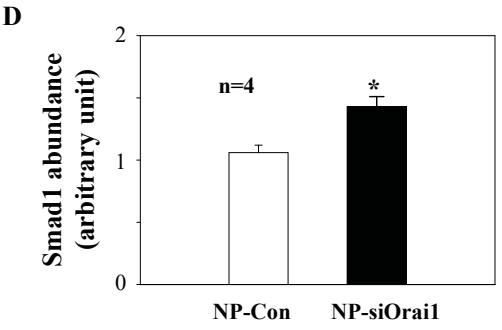
D
Smad1 abundance (arbitrary unit)
2
1
0
n=4
*
NP-Con
NP-siOrai1

Fig. 8

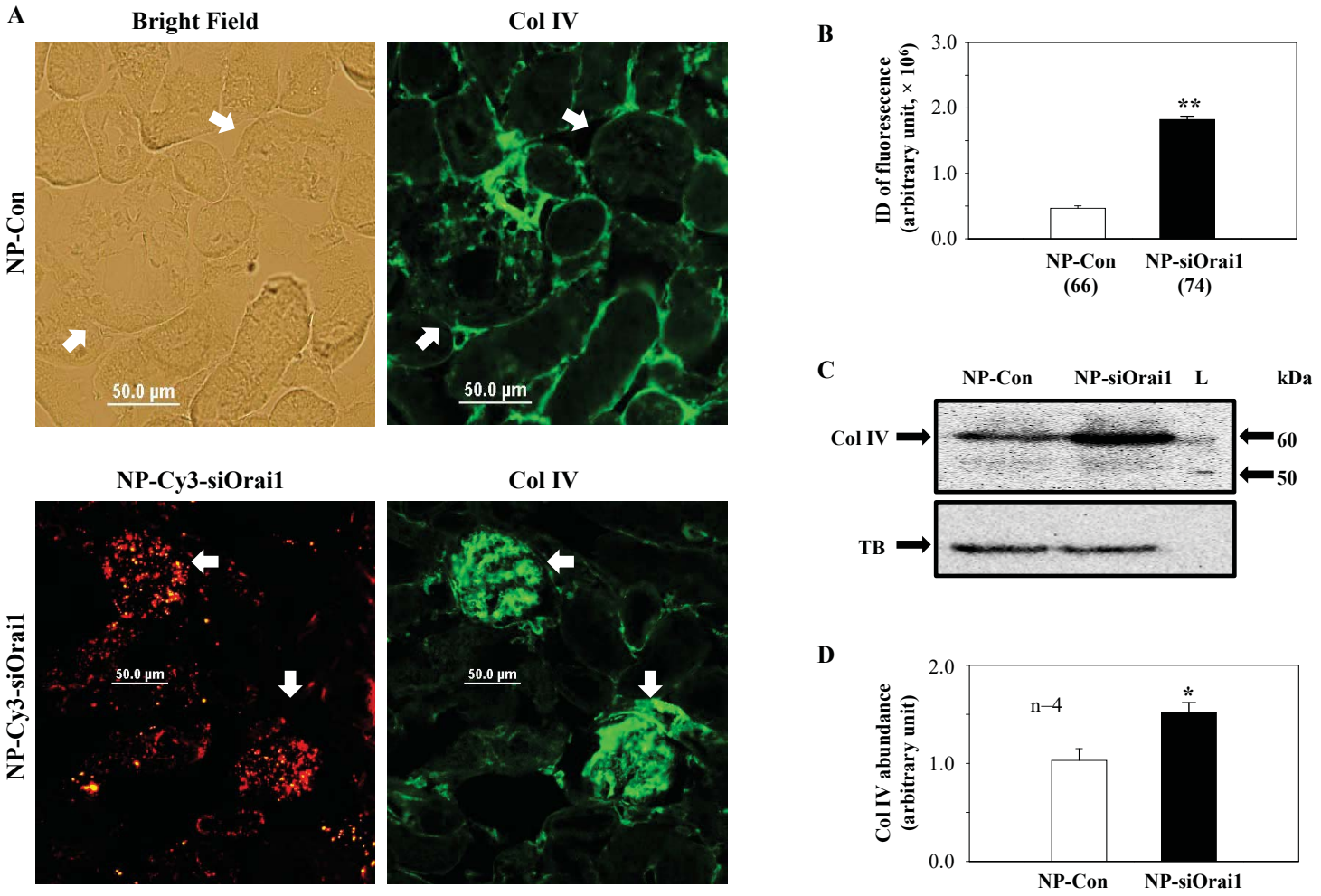
A
Bright Field
Col IV
NP-Con
50.0 μm
50.0 μm
NP-Cy3-siOrai1
Col IV
NP-Cy3-siOrai1
50.0 μm
50.0 μm
B
ID of fluoresecence (arbitrary unit, × 10⁶)
3.0
2.0
1.0
0.0
**
NP-Con (66)
NP-siOrai1 (74)
C
NP-Con
NP-siOrai1
L
kDa
Col IV
60
50
TB
D
Col IV abundance (arbitrary unit)
2.0
1.0
0.0
n=4
*
NP-Con
NP-siOrai1